*Proc. CIBSE A: Building Serv. Eng. Res. Technol.* **19**(2) 73–77 (1998) Printed in Great Britain B427



**Summary** A study of air movement and aerosol particle distribution and migration in a ventilated two-zone chamber is presented. The comparisons of average particle concentration decay between numerical results and measured data are generally satisfactory and acceptable. It can be concluded that the particle distribution and migration are mainly influenced by the airflow pattern and ventilation rates.

# Airborne particles in a ventilated room: Prediction and measurement

**Weizhen Lu**†§BSc MPhil PhD **Andrew T Howarth**†BSc MPhil PhD CEng MCIBSE MIMechE **Nor Adam**‡BSc MPhil PhD and **Saffa B Riffat**‡BSc MPhil PhD MCIBSE MIMechE MASHRAE
†School of the Built Environment, De Montfort University, Leicester LE1 9BH, UK
‡School of Architecture, University of Nottingham, Nottingham NG7 2RD, UK

Received 28 October 1996, in final form 30 October 1997

## List of symbols

$C$ Concentration (mg m$^{-3}$)
$C_D$ Drag factor
$C_p$ Average particle concentration in each zone ($\mu$g m$^{-3}$)
$d$ Diameter ($\mu$m)
$F$ External force (N m$^{-3}$)
$F_D$ Drag force on particle (N m$^{-3}$)
$F_B$ Body force on particle (N m$^{-3}$)
$g$ Gravitational acceleration (m s$^{-2}$)
$H$ Height (m)
$k$ Kinetic energy of turbulence ($= {}^1/_2 u_i^2$) (m$^2$s$^{-2}$)
$L$ Length (m)
$m$ Mass (kg)
$m_z$ Mass of suspended particles in each zone ($\mu$g)
$N_{pd}$ Number of particles deposited in each zone
$N_{pe}$ Number of particles extracted from room
$N_{pm}$ Number of particles migrating between zones
$R_d$ Average particle deposition rate in each zone (h$^{-1}$)
$R_{exc}$ Average particle exchange rate in room (h$^{-1}$)
$R_{ext}$ Average particle extraction rate in room (h$^{-1}$)
$Re_p$ Particle Reynolds number ($\rho V_R d_p/\mu$)
$S_{\phi i}$ Source term
$T_{trk}$ Total particle tracking time (min or h)
$T_i$ Suspension period of sample particles (min)
$t$ Time (s or min)
$u$ Velocity in $x$ direction (m s$^{-1}$)
$v$ Velocity in $y$ direction (m s$^{-1}$)
$V$ Volume of room (m$^3$)
$V_z$ Volume of each zone (m$^3$)
$V_R$ Relative velocity between air and particle (m s$^{-1}$)
$w$ Velocity in $z$ direction (m s$^{-1}$)
$W$ width (m)
$x, y, z$ Co-ordinates
$\Gamma$ Effective exchange coefficient
$\varepsilon$ Turbulent energy dissipation rate
$\rho$ Density (kg m$^{-3}$)
$\Phi_i$ Dependent variable
$\mu$ Dynamic viscosity (kg m$^{-1}$·s$^{-1}$)

*Subscripts*

$i$ $i$th direction
i Inlet
o Opening
p Particle

§Present address: Structural Dynamics Research Centre, Department of Building and Construction, City University of Hong Kong, 83 Tat Chee Avenue, Kowloon Tong, Kowloon, Hong Kong, China

## 1 Introduction

Aerosol particles are regarded as one of the main pollutant sources in the indoor environment. They arise from a combination of indoor sources (e.g. cigarette smoke, building materials, personal products, etc.) and outdoor sources (e.g. car exhaust emissions, coal and oil combustion, pollen, road dust etc.) which may enter the building through ventilation system. Previous studies show that particle movement in ventilated multizone areas is a complicated phenomenon and is influenced by many factors, such as airflow pattern, geometric configurations, particle properties, ventilation conditions, supply and exhaust diffuser locations, internal partitions, thermal buoyancy due to the heat generated by occupants and/or equipment[1–5] etc. Another important phenomenon of particle movement in multizone areas is particle migration between zones due to momentum and thermal imbalances between zones. This means that the pollutant source in one zone may be transferred to others by particle migration. Particles suspended in the air or migrating between zones have a significant influence on human health (they may be inhaled by the occupants and deposited in the nasal passage with potentially harmful effects) and indoor air quality. The indoor air quality in multizone buildings has received much attention in recent years.

However, the knowledge of aerosol particle behaviour in the multizone spaces is still limited. The research presented in this paper uses a CFD method to predict airflow and aerosol particle distribution in a full-scale ventilated two-zone chamber and to compare the numerical results with the corresponding experimental data. The purposes of the study are to obtain information about the aerosol particle distribution, migration and deposition in the space and to analyse the air movement.

## 2 Case study

### 2.1 Parameters of experiment

The chamber, of two zones, has dimensions 5 m (length) × 2.4 m (height) × 3 m (width) as shown in Figure 1. The room is divided into two equal zones by a partition with a small opening. The opening is located on the centreline of the chamber. The thickness of the partition can be ignored compared with the room size. The study includes numerical computation and experimental measurements. The air flow is assumed to be steady, incompressible and isothermal. The

**Table 1** Parameters of cases

| Case no. | $L$(m) | $H$(m) | $W$(m) | $L_i$(m) | $H_i$(m) | $W_i$(m) | $H_o$(m) | $W_o$(m) | Ventilation rate ($h^{-1}$) | $R_{ei}$ | No. of iterations | Area ratio of opening to partition |
|---|---|---|---|---|---|---|---|---|---|---|---|---|
| 1 | 5 | 2.4 | 3 | 0.15 | 0.5 | 1.0 | 0.3 | 0.7 | 11.566 | 1285 | 4000 | 0.03 |
| 2 | 5 | 2.4 | 3 | 0.15 | 0.5 | 1.0 | 0.3 | 0.7 | 12.708 | 1413 | 4000 | 0.03 |

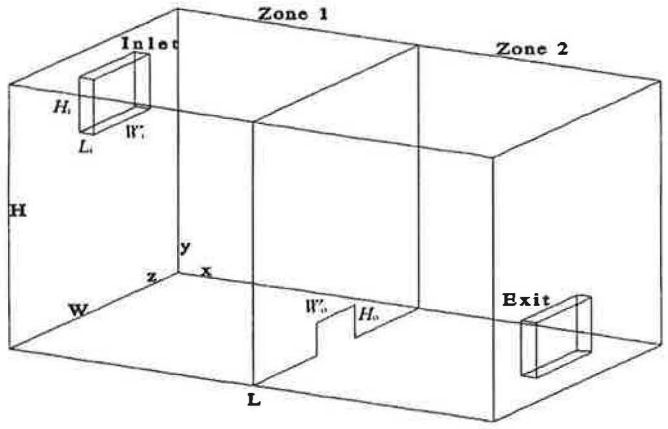


**Figure 1** Geometric configuration

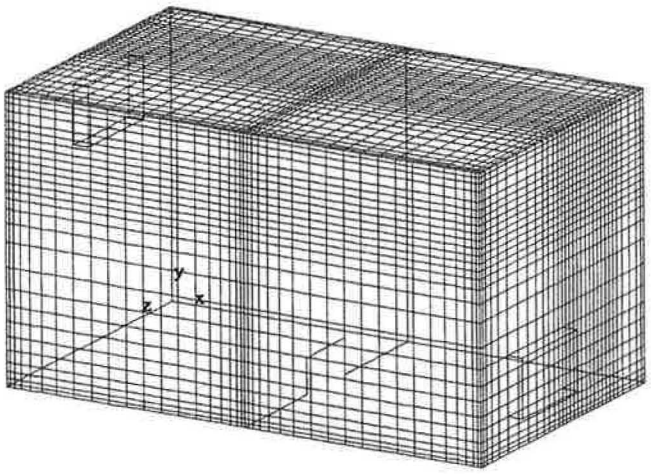

**Figure 2** Mesh scheme

room air temperature is 20°C. The chamber is assumed to be well sealed and the only exit for the room air is through the exhaust section. Table 1 shows the relevant parameters for two ventilation cases.

### 2.2 *Numerical simulations*

Computational fluid dynamics is employed in the numerical simulations. The Eulerian mathematical model is used to represent the continuous fluid flow and the Lagrangian particle transport model is used to track the particle movement. The equation sets are listed below.

The general governing equation for the continuous fluid is

$$\partial(\rho\Phi_i)/\partial t + \mathrm{div}(\rho U\Phi_i) - \mathrm{div}(\Gamma_{\Phi i}\nabla\Phi_i) = S_{\Phi i} \quad (1)$$

The equation set for particle motion is

$$m\mathrm{d}u/\mathrm{d}t = F \quad (2)$$

$$F_D = (1/8)\pi d_p^2 \rho C_D |V_R| V_R \quad (3)$$

$$F_B = (1/6)\pi d_p^3(\rho_p - \rho)g \quad (4)$$

$$C_D = (24/\mathrm{Re}_p)(1 + 0.15\mathrm{Re}_p^{0.687}) \quad (5)$$

$$\mathrm{Re}_p = \rho |V_R| d_p/\mu \quad (6)$$

Both equation sets are solved by using the CFDS-FLOW3D package. Here $\Phi_i$ represents the velocity field ($u$, $v$, $w$) and the turbulent variables $k$ and $\varepsilon$. A standard $k$–$\varepsilon$ model is applied to describe the nature of the turbulence. All particles are assumed to be spherical. Particles do not rebound on making contact with the solid surfaces. The room is divided into 40 × 28 × 30 cells (i.e. control volumes). The supply section is divided into 3 × 8 × 14 cells, while 3 × 4 × 8 cells constitute the exhaust section. A refined mesh is established near all walls of the chamber including the partition (see Figure 2). All simulations were carried out on a SUN-SPARC2 workstation.

## 3 Initial and boundary conditions

### 3.1 *Boundary conditions for airflow*

The following boundary conditions are specified for the continuous phase.

— All variables upstream of the flow domain are set up according to the principles of the Dirichlet boundary condition[7]. The main flow is specified as entering the chamber with a uniform velocity calculated according to the respective ventilation rate for each case. The quantities $k$ and $\varepsilon$ at the inlet are based on the mean flow characteristics at the inlet, i.e. the inlet velocities[7].

— A non-slip condition at the solid wall is applied to the velocities. The wall function is employed to describe the turbulent properties near the wall.

— Neumann boundary conditions[7] are applied at the outlet to satisfy the conservation of mass.

### 3.2 *Initial conditions for particle tracking*

The initial conditions for particle tracking include the starting positions and initial velocities of the particles. The particle density is that of oil smoke, i.e. $\rho_p$ = 865.0 kg $m^{-3}$ and are divided equally into five size groups from 1 to 5 $\mu$m. Those particles which are less than 1$\mu$m across are included in the 1 $\mu$m size group. In the experimental work, smoke particles are initially injected into zone 1 and mixed well. They are assumed to be uniformly distributed in the initial measurement area, i.e. zone 1 (Figure 3). The total mass of particles injected into zone 1 in each case is determined according to the experimental data. The periods for which the particles are tracked are the same as experimental monitoring periods correspondingly. The total particle sample is 800, with 160 in each size group. Tables 2 and 3 give the particle parameters for each case.

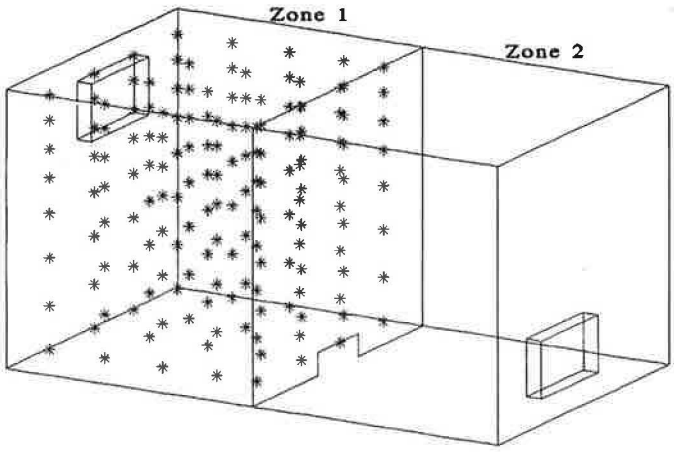


**Figure 3** Initial positions of sample particles

**Table 2** Particle parameters for Case 1 (11.566 $h^{-1}$)

| Size $d_p$ ($\mu$m) | Particle mass represented by each sample particle ($\mu$g) | Number of sample particles | Tracking period $T_{trk}$ (min; h) |
|---|---|---|---|
| 1, 2, 3, 4 and 5 | 5 × 149.4 | 5 × 160 | 35; 0.5833 |

**Table 3** Particle parameters for Case 2 (12.708 $h^{-1}$)

| Size $d_p$ ($\mu$m) | Particle mass represented by each sample particle ($\mu$g) | Number of sample particles | Tracking period $T_{trk}$ (min; h) |
|---|---|---|---|
| 1, 2, 3, 4 and 5 | 5 × 118.17 | 5 × 160 | 24; 0.4 |

### *2.4 Experimental procedure*

The experimental work was carried out in an environmental chamber. A variable-speed fan supplied fresh air to the chamber via the inlet diffuser. The air was removed from the chamber via the exit diffuser. $SF_6$ tracer gas and oil-smoke were injected into the chamber with all the dampers, interzonal openings and fans shut. 10 minutes were allowed for the tracer gas and oil-smoke to mix with the air in the chamber. Once a uniform concentration of tracer gas and smoke particles had been achieved in the chamber, dampers at the respective diffusers and interzonal opening were opened and the fan switched on. At the same time, monitoring of the concentration of tracer gas and smoke particles at the centre of each zone began, using an infrared gas analyser and an infrared particle monitor respectively. The measured data represent the corresponding average particle concentrations in each zone.

## 3 Results and analysis

### *3.1 Airflow patterns in two-zone room*

Figures 4 and 5 show the simulated airflow patterns in different planes for Case 1 by computational fluid dynamics. The supply air forms a jet-like flow after the supply section. The jet flow splits at the partition surface, and creates a larger air circulation below the jet core and two separation vortexes at both top corners in zone 1 (Figure 4). A jet-like flow is also produced at floor level in zone 2 because of the discharge effect of the interzonal opening (see Figure 5). The discharge effect also induces air circulation in that area. It is interesting to notice that the recirculation centres are not at the centre of each zone due to the jet effect (Figures 4 and 5). These airflow

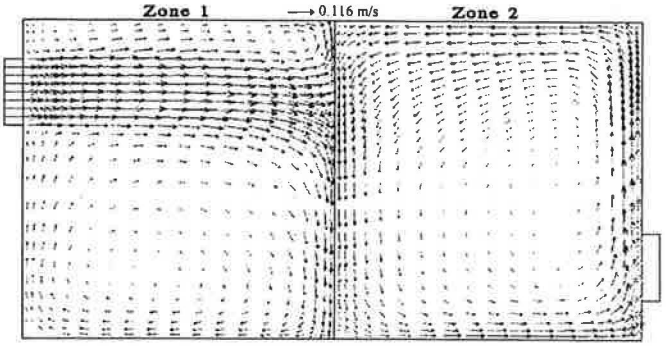


**Figure 4** Airflow pattern crossing central supply section (Case 1)

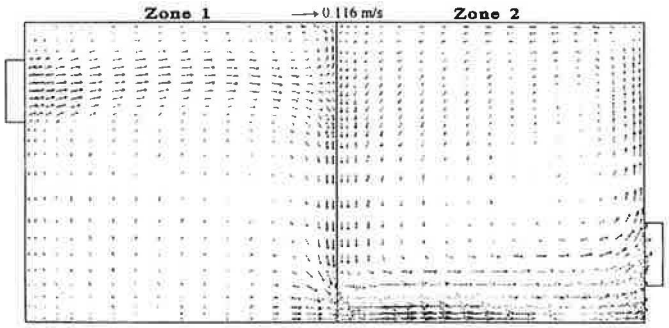


**Figure 5** Airflow pattern in centre-line plane (Case 1)

patterns will affect the particle distribution and migration in both zones. The air movement for case 2 is similar to that for case 1.

### *3.2 Particle movement and distribution in two-zone room*

The following parameters are defined:

Average particle concentration in each zone:

$$C_p = m_z/V_z \tag{7}$$

Average particle deposition, exchange and extraction rates for two-zone chamber:

Average particle deposition rate in each zone:

$$R_d = m_p N_{pd}/\rho_p T_{trk} V_z \tag{8}$$

Average particle exchange rate in room:

$$R_{exc} = m_p N_{pm}/\rho_p T_{trk} V \tag{9}$$

Average particle extraction rate in room:

$$R_{ext} = m_p N_{pe}/\rho_p T_{trk} V \tag{10}$$

The variation of average particle concentration with time can be obtained according to equation 7. Average particle concentration by computation and experiment for the two cases are compared in Figures 6–9. Both particle concentrations decay with time. The numerical results show reasonably good agreement with the measured data, especially in the first ten minutes of the tracking periods. The assumption that measurements at the centre points represent the average concentration is relevant to the comparison between computed and measured data, between which there are some discrepancies. This can be explained as follows. The assumption that the particle mass is uniformly divided between size groups is unrealistic. Particle rebound is neglected in the simulations; this may contribute to the errors.

Figures 10–13 describe the particle distribution, migration and deposition for the two cases. The masses of suspended particles in zone 1 decline continuously with time in both

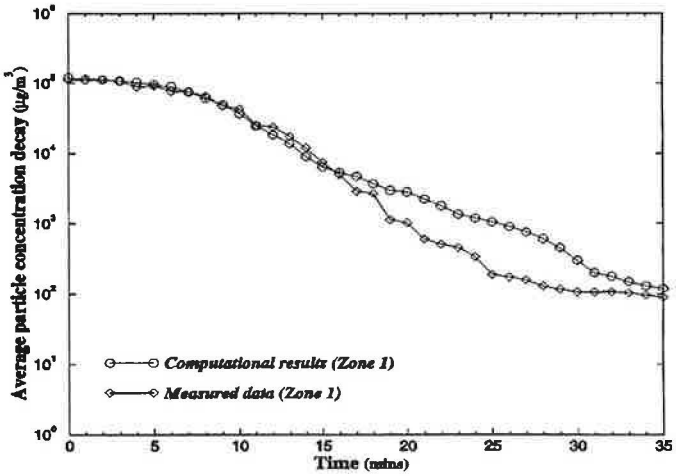


Figure 6 Average particle concentration decay in Zone 1 (Case 1, 11.566 $h^{-1}$)

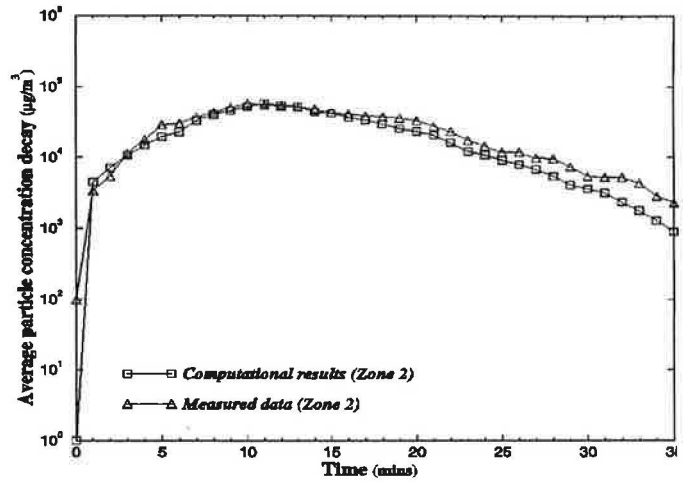


Figure 7 Average particle concentration decay in Zone 2 (Case 1, 11.566 $h^{-1}$)

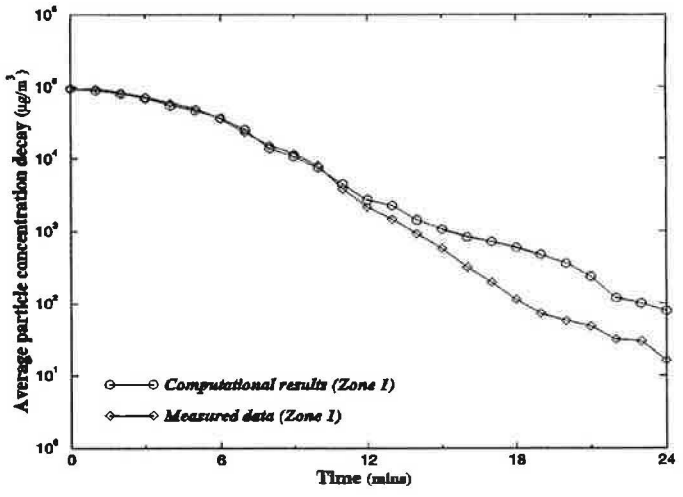


Figure 8 Average particle concentration decay in Zone 1 (Case 2, 12.708 $h^{-1}$)

cases, whereas the masses of suspended particles in zone 2 first increase and then decrease with time. Particle migration occurs mainly within the first few minutes after the interzonal connection is opened; from Figures 10 and 12, 15 minutes for Case 1 and 10 minutes for Case 2. This phenomenon may be termed 'massive particle migration'. After the massive migration period, the masses of particles migrating do not change much with time. This means that the rates of particle migration reduce rapidly after the massive migration period. Figures 10–13 also show that the masses of particles deposited

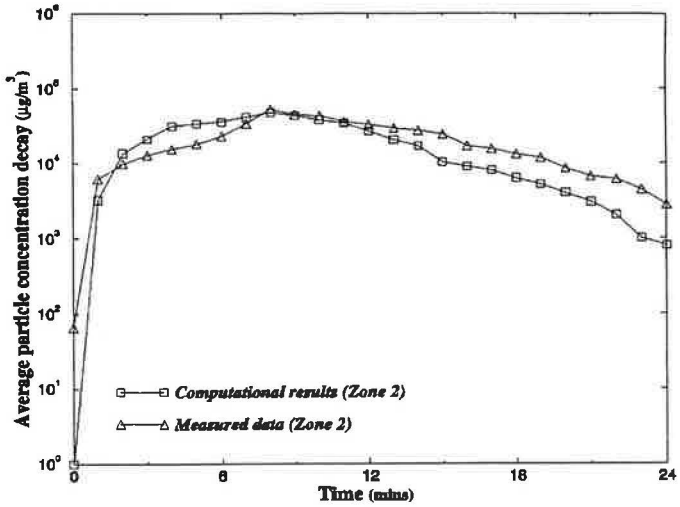


Figure 9 Average particle concentration decay in Zone 2 (Case 2, 12.708 $h^{-1}$)

on the internal surfaces in both zones and extracted from zone 2 generally increase with time. From Figures 10–13, it can be seen that more particles are suspended in zone 2 than in zone 1 after the first 10 minutes. This means that the particle concentration level in zone 2 is sensitive to upstream airflow and particle migration.

Figure 14 shows the average particle deposition, exchange and extraction rates under various ventilation conditions.

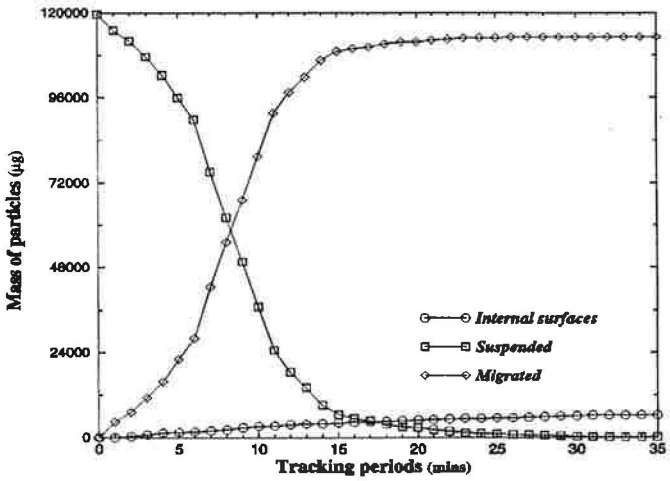


Figure 10 Particle distribution in Zone 1 (Case 1, 11.566 $h^{-1}$)

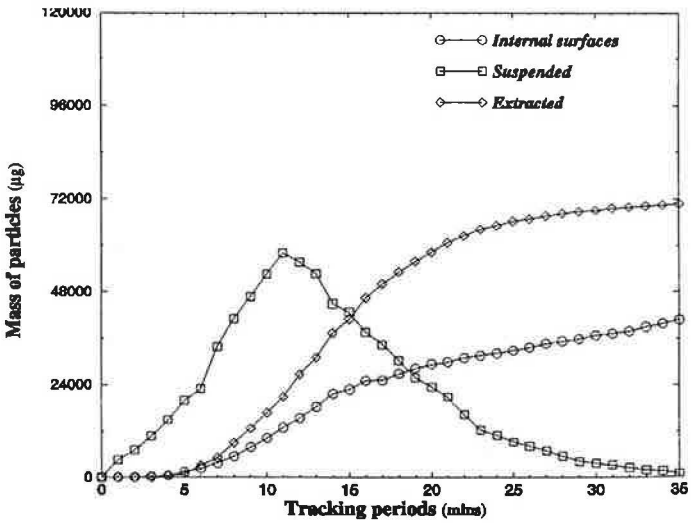


Figure 11 Particle distribution in Zone 2 (Case 1, 11.566 $h^{-1}$)

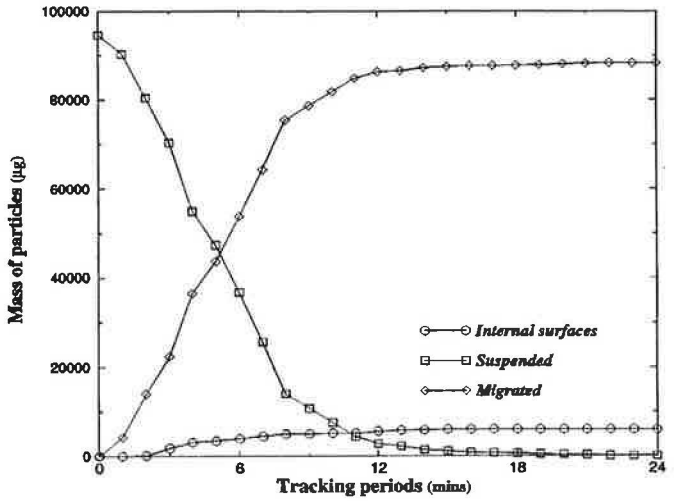


**Figure 12** Particle distribution in Zone 1 (Case 2, 12.708 $h^{-1}$)

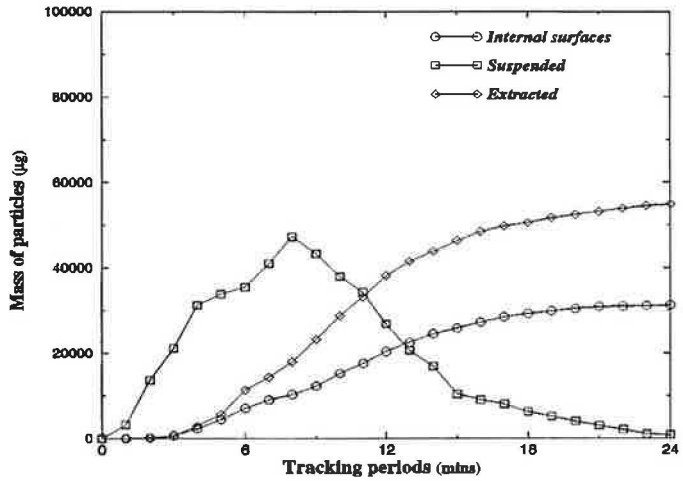


**Figure 13** Particle distribution in Zone 2 (Case 2, 12.708 $h^{-1}$)

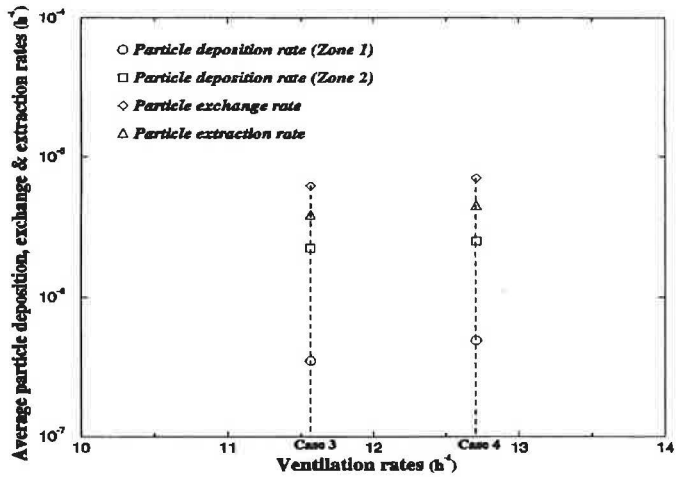


**Figure 14** Average particle deposition, exchange and extraction rates for the two cases

These values increase as the ventilation rate increases. this implies that the ventilation conditions do influence the airborne particle distribution and hence the indoor air quality. Figure 15 shows tracking routes for five sample particles throughout the ventilated space. Large particles ($d_p > 3$ $\mu$m) deposit faster than small particles. Particles suspended in the

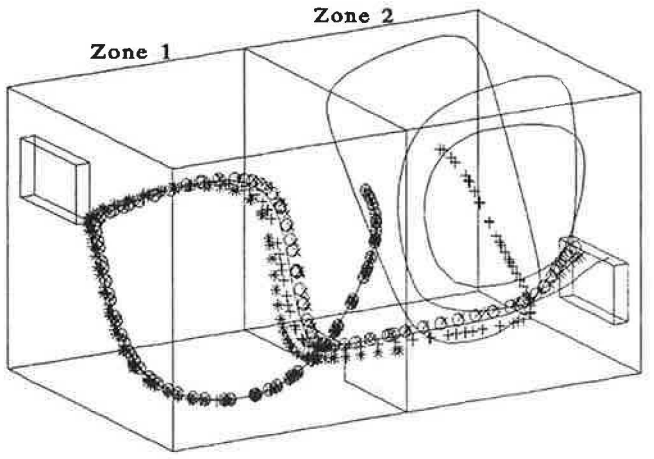


**Figure 15** Five sample particle tracking routes (Case 1, 11.566 ac $h^{-1}$) — 1$\mu$m (19 min); + 2$\mu$m (8 min); O 3$\mu$m (5 min); × 4$\mu$m (4.2 min); ⋆ 5 $\mu$m (3.2 min)

room space (i.e. small ones) significantly influence the particle concentration level and indoor air quality.

## 4 Conclusions

The following conclusions emerge from a CFD analysis of airflow and aerosol particle distribution, migration and deposition in a ventilated two-zone area:

— Computations and measurements of average particle concentration decay generally agree well.

— Particle movement and distribution are greatly influenced by the airflow pattern and ventilation rate.

— The indoor air quality in a multizone area is affected by particle deposition, migration and suspension. The air quality in zone 2, in this study, is more sensitive to particle migration and suspension than that in zone 1.

## Acknowledgement

This work was sponsored by the United Kingdom Engineering and Physical Science Research Council.

## References

1 Nazaroff W, Ligock M P, Ma T and Cass G R Particle deposition in museum: Comparison of modelling and measurement results *Aerosol Sci. Technol.* **13** 332–348 (1990)

2 Xu M, Nematollahi M, Sextro R G, Gadgi A J and Nazaroff W W Deposition of tobacco smoke particle in a low ventilated room *Aerosol Sci. Technol.* **20** 194–206 (1994)

3 Lu W and. Howarth A T Indoor aerosol particle deposition and distribution: Numerical analysis for a one-zone ventilation system *Building Serv. Eng. Res. Technol.* **16**(3) 141–147 (1995)

4 Lu W and Howarth A T Numerical analysis of indoor aerosol particle deposition and distribution in two-zone ventilation system *Building and Environment* **31**(1) 41–50 (1996)

5 Adam K W, Cheong X Y, Riffat S B and Shao L Measurement and modelling of aerosol particle flow in an environmental chamber *Proc. CIBSE Conf., Buxton, UK* (Oct 1994)

6 Lu W,. Howarth A T, Adam N and Riffat S B Modelling and measurement of airflowand aerosol particle distribution in a ventilated two-zone chamber *Building and Environment* **31**(5) 417–423 (1996)

7 CFDS-FLOW3D Guide (United Kingdom Atomic Energy Authority Harwell Laboratory) (1994)